Inorg. Chem. **2003**, *42*, 785–795

Inorganic Chemistry
Article

Ruthenium(II) Complexes Containing 8-(Dimethylphosphino)quinoline (Me_2Pqn): Preparation, Crystal Structures, and Electrochemical and Spectroscopic Properties of $[Ru(bpy\ or\ phen)_{3-n}(Me_2Pqn)_n](PF_6)_2$ (bpy = 2,2′-Bipyridine; phen = 1,10-Phenanthroline; n = 1, 2, or 3)

Takayoshi Suzuki,*,† Takashi Kuchiyama,† Shinobu Kishi,‡ Sumio Kaizaki,† Hideo D. Takagi,§ and Masako Kato‡

Department of Chemistry, Graduate School of Science, Osaka University, Toyonaka 560-0043, Japan, Division of Material Science, Graduate School of Human Culture, Nara Women's University, Nara 630-8506, Japan, and Department of Chemistry, Graduate School of Science, Nagoya University, Chikusa, Nagoya 464-8602, Japan

Received May 13, 2002

Several new ruthenium(II) complexes containing 8-(dimethylphosphino)quinoline (Me_2Pqn) were synthesized, and their structures and electrochemical/spectroscopic properties have been investigated. In addition to the mono-(Me_2Pqn) complex $[Ru(bpy\ or\ phen)_2(Me_2Pqn)](PF_6)_2$ (**1** or **1′**; bpy = 2,2′-bipyridine; phen = 1,10-phenanthroline), the geometrical isomers *trans(P)*- and C_1-$[Ru(bpy)(Me_2Pqn)_2](PF_6)_2$ (***tP*-2** and ***C*₁-2**) and *mer*- and *fac*-$[Ru(Me_2Pqn)_3](PF_6)_2$ (***m*-3** and ***f*-3**) were also selectively synthesized and isolated. It was found that complexes ***tP*-2** and ***m*-3** were converted quantitatively to the corresponding ***C*₁-2** and ***f*-3** isomers, respectively, by irradiation of light corresponding to the MLCT transition energy. The strong *trans* influence of the Me_2P– donor group of Me_2Pqn was confirmed by the X-ray structural analyses for **1**, ***tP*-2**, ***m*-3**, and ***f*-3**. Cyclic voltammetry of a series of complexes, $[Ru(bpy)_3](PF_6)_2$, **1**, ***C*₁-2**, and ***f*-3**, exhibited a reversible one-electron oxidation wave and two or three one-electron reduction waves. The oxidation potentials of the complexes gave a large positive shift with increasing number of coordinated Me_2Pqn molecules, indicating a larger π-acceptability of the Me_2P– group compared with bpy or qn. Complex ***f*-3** in EtOH/MeOH (4:1) glass at 77 K exhibited an intense long-lived (τ = 920 μs) emission arising from the quinoline-based $^3(\pi-\pi^*)$ excited state. In contrast, the mixed-ligand complexes **1**, **1′**, and ***C*₁-2** showed a characteristic dual emission, giving a double-exponential emission decay, and the dual emission originates from both the bpy-based ^{3}MLCT and the quinoline-based $^3(\pi-\pi^*)$ emitting states.

Introduction

The compounds of 8-quinolylphosphines (Chart 1)[1−6] can act as asymmetric bidentate ligands bearing two donor groups with different electronic characters, a phosphino (RR′P−) group with a strong π-acidity and a quinoline group as a moderate σ-donor. In addition to the steric advantage to form a strain-free five-membered chelate ring,[1,2a] such an electronic differentiation[7] of these ligands may stabilize unusual oxidation states or coordination geometries upon coordination to

Chart 1. 8-Quinolylphosphines

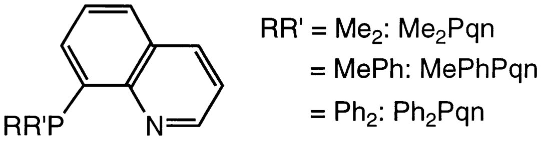

---

* Author to whom correspondence should be addressed. E-mail: suzuki@chem.sci.osaka-u.ac.jp.

† Osaka University.

‡ Nara Women's University.

§ Nagoya University.

(1) Suzuki, T.; Kashiwabara, K.; Fujita, J. *Bull. Chem. Soc. Jpn.* **1995**, *68*, 1619−1626.

(2) (a) Allen, D. G.; McLaughlin, G. M.; Robertson, G. B.; Steffen, W. L.; Salem, G.; Wild, S. B. *Inorg. Chem.* **1982**, *21*, 1007−1014. (b) Salem, G.; Wild, S. B. *Inorg. Chem.* **1992**, *31*, 581−586.

(3) Hudali, H. A.; Kingston, J. V.; Tayim, H. A. *Inorg. Chem.* **1979**, *18*, 1391−1394.

(4) Issleib, K.; Hörnig, K. *Z. Anorg. Allg. Chem.* **1972**, *389*, 263−268.

(5) Wehman, P.; van Donge, H. M. A.; Hagos, A.; Kamer, P. C. J.; van Leeuwen, P. W. N. M. *J. Organomet. Chem.* **1997**, *535*, 183−193.

(6) (a) Feltham, R. D.; Metzger, H. G. *J. Organomet. Chem.* **1971**, *33*, 347−355. (b) Issleib, K.; Haftendorn, M. *Z. Anorg. Allg. Chem.* **1970**, *376*, 79−86.

10.1021/ic020344l CCC: $25.00

the transition metals, and therefore, the complexes with these ligands may have novel structural, spectroscopic, and photophysical properties. However, only a limited number of studies have been reported for the transition-metal complexes of 8-quinolylphosphines to date.[1−5] Several transition-metal complexes with 8-(diphenylphosphino)quinoline (Ph_2Pqn) have been reported, although their structures and properties are not investigated in detail.[3−5] While Wild et al. reported excellent results concerning diastereoisomerism of palladium(II) and platinum(II) complexes containing 8-(methylphenylphosphino)quinoline (MePhPqn) or its arsine derivative,[2] no complex of other metal ions with the chiral phosphine has been reported. As 8-(dimethylphosphino)quinoline (Me_2Pqn) with a Me_2P- donor group exhibits a stronger σ-donicity and a smaller steric bulk than the other quinoline ligands with Ph_2P- and MePhP− groups, various kinds of transition-metal ions are expected to be stabilized with this ligand. However, there has been no example of such metal complexes with Me_2Pqn, except for our previous study on the mononuclear palladium(II) and dinuclear palladium(I) complexes.[1] To investigate the coordination chemistry of Me_2Pqn in more detail, we have synthesized the novel mixed-ligand ruthenium(II) complexes of Me_2Pqn with either 2,2′-bipyridine (bpy) or 1,10-phenanthroline (phen) coligands.

Ruthenium(II) polypyridine complexes have been intensively investigated to date not only to accumulate knowledge of the fundamental coordination chemistry, electrochemistry, photochemisty, and photophysics of these complexes,[8−10] but also to seek the potential applicability of these complexes to energy conversion, luminescent sensors, electroluminescence displays, and biotechnology.[11−14] To develop new types of chemical materials suitable for such applications, a great number of mixed-ligand ruthenium(II) polypyridine complexes have been synthesized to tune the ground-state and/or the excited-state properties.[8,9,15−24] Ruthenium(II) phosphine complexes have also been extensively studied from the viewpoints of high catalytic abilities[25] and potential uses as organometallic molecular wires, low-dimensional conductors, and nonlinear optical materials.[26] However, it is rather surprising that only a few studies have been carried out for ruthenium(II) complexes with polypyridine and phosphine ligands.[21−24]

In this paper, we describe the preparation, structural characterization, and electrochemical and spectroscopic properties of a series of ruthenium(II) complexes containing Me_2Pqn, $[Ru(bpy)_{3-n}(Me_2Pqn)_n](PF_6)_2$ ($n = 1$ (**1**), 2 (**2**), and 3 (**3**); Chart 2), together with the analogous phen complex $[Ru(phen)_2(Me_2Pqn)](PF_6)_2$ (**1′**).

Experimental Section

Materials and General Procedures. The phosphines Me_2Pqn[1] and 1,2-bis(dimethylphosphino)benzene (dmpb)[27] and the Ru^{II} complexes *cis*-$[RuCl_2(bpy)_2]\cdot 2H_2O$,[28] *cis*-$[RuCl_2(phen)_2]\cdot 2H_2O$,[24] *cis*-$[RuCl_2(dmso)_4]$,[29] and $[Ru(bpy)_2(phen)](PF_6)_2$[30] were prepared according to the literature methods. All reactions were handled under an atmosphere of argon using standard Schlenk techniques until such time that air-stable ruthenium(II) phosphine complexes

---

(7) Espinet, P.; Soulantica, K. *Coord. Chem. Rev.* **1999**, *193−195*, 499−556.

(8) Juris, A.; Balzani, V.; Barigelletti, F.; Campagna, S.; Belser, P.; von Zelewsky, A. *Coord. Chem. Rev.* **1988**, *84*, 85−277.

(9) (a) Lever, A. B. P. *Inorg. Chem.* **1990**, *29*, 1271−1285. (b) Dodsworth, E. S.; Lever, A. B. P. *Chem. Phys. Lett.* **1986**, *124*, 152−158.

(10) Roundhill, D. M. *Photochemistry and Photophysics of Metal Complexes*; Plenum Press: New York, 1994; Chapter 5.

(11) (a) Bignozzi, C. A.; Schoonover, J. R.; Scandola, F. *Prog. Inorg. Chem.* **1997**, *44*, 1−95. (b) Clark, C. D.; Hoffman, M. Z. *Coord. Chem. Rev.* **1997**, *159*, 359−373. (c) De Cola L.; Belser, P. *Coord. Chem. Rev.* **1998**, *177*, 301−346. (d) Ward, M. D.; Barigelletti, F. *Coord. Chem. Rev.* **2001**, *216−217*, 127−154.

(12) (a) Beer, P. D. *Acc. Chem. Res.* **1998**, *31*, 71−80. (b) Demas, J. N.; DeGraff, B. A. *Coord. Chem. Rev.* **2001**, *211*, 317−351.

(13) (a) Wu, A.; Yoo, D.; Lee, J.-K.; Rubner, M. F. *J. Am. Chem. Soc.* **1999**, *121*, 4883−4891. (b) Gao, F. G.; Bard, A. J. *J. Am. Chem. Soc.* **2000**, *122*, 7426−7427.

(14) (a) Barton, J. K. *Science* **1986**, *233*, 727−734. (b) Turro, C.; Bossmann, S. H.; Jenkins, Y.; Barton, J. K.; Turro, N. J. *J. Am. Chem. Soc.* **1995**, *117*, 9026−9032. (c) Gray, H. B.; Winkler, J. R. *Annu. Rev. Biochem.* **1996**, *65*, 537−561. (d) Guerzo, A. D.; Kirsch-DeMesmaeker, A. *Inorg. Chem.* **2002**, *41*, 938−945.

(15) Juris, A.; Barigelletti, F.; Balzani, V.; Belster, P.; von Zelewsky, A. *Inorg. Chem.* **1985**, *24*, 202−206.

(16) (a) Ross, H. B.; Boldaji, M.; Rillema, D. P.; Blanton, C. B.; White, R. P. *Inorg. Chem.* **1989**, *28*, 1013−1021. (b) Kawanishi, K.; Kitamura, N.; Tazuke, S. *Inorg. Chem.* **1989**, *28*, 2968−2975. (c) Zakeeruddin, S. M.; Nazeeruddin, Md. K.; Humphry-Baker, R.; Grätzel, M.; Shklover, V. *Inorg. Chem.* **1998**, *37*, 5251−5259. (d) Krause, R. A. *Inorg. Chim. Acta* **1977**, *22*, 209−213. (e) Yamanari, K.; Nozaki, T.; Fuyuhiro, A.; Kushi, Y.; Kaizaki, S. *J. Chem. Soc., Dalton Trans.* **1999**, 2851−2856. (f) Aydin, N.; Schlaepher, C.-W. *Polyhedron* **2001**, *20*, 37−45. (g) Norrby, T.; Börje, A.; Åkermark, B.; Hammarström, L.; Alsins, J.; Lashgari, K.; Norrestam, R.; Mårtensson, J.; and Stehagen, G. *Inorg. Chem.* **1997**, *36*, 5850−5858.

(17) (a) Blakley, R. L.; DeArmond, M. K. *J. Am. Chem. Soc.* **1987**, *109*, 4895−4901. (b) Morris, D. E.; Ohsawa, Y.; Segers, D. P.; DeArmond, M. K.; Hanck, K. W. *Inorg. Chem.* **1984**, *23*, 3010−3017. (c) Nagao, N.; Mukaida, M.; Miki, E.; Mizumachi, K.; Ishimori, T. *Bull. Chem. Soc. Jpn.* **1994**, *67*, 2447−2453.

(18) (a) Keyes, T. E.; O'Connor, C.; Vos, J. G. *Chem. Commun.* **1998**, 889−890. (b) Fanni, S.; Keyes, T. E.; O'Connor, C.; Hughes, H.; Wang, R.; Vos, J. G. *Coord. Chem. Rev.* **2000**, *208*, 77−86. (c) Keyes, T. E.; O'Connor, C. M.; O'Dwyer, U.; Coates, C. G.; Callaghan, P.; McGarey, J. J.; Vos, J. G. *J. Phys. Chem. A* **1999**, *103*, 8915−8920.

(19) (a) Wilson, G. J.; Launikonis, A.; Sasse, W. H. F.; Mau, A. W.-H. *J. Phys. Chem. A* **1997**, *101*, 4860−4816. (b) Simon, J. A.; Curry, S. L.; Schmehl, R. H.; Schatz, T. R.; Piotrowiak, P.; Jin, X.; Thummel, R. P. *J. Am. Chem. Soc.* **1997**, *119*, 11012−11022. (c) Guerzo, A. D.; Leroy, S.; Fages, F.; Schmehl. R. H. *Inorg. Chem.* **2002**, *41*, 359−366. (d) Tyson, D. S.; Luman, C. R.; Zhou, X.; Castellano, F. N. *Inorg. Chem.* **2001**, *40*, 4063−4071.

(20) Warren, J. T.; Chen, W.; Johnston, D. H.; Turro, C. *Inorg. Chem.* **1999**, *38*, 6187−6192.

(21) Keene, F. R.; Snow, M. R.; Stephenson, P. J.; Tiekink, E. R. T. *Inorg. Chem.* **1988**, *27*, 2040−2045.

(22) (a) Sullivan, B. P.; Salmon, D. J.; Meyer, T. J. *Inorg. Chem.* **1978**, *17*, 3334−3341. (b) Casper, J. V.; Meyer, T. J. *Inorg. Chem.* **1983**, *22*, 2444−2453. (c) Walsh, J. L.; Durham, B. *Inorg. Chem.* **1982**, *21*, 329−332. (d) Blake, A. J.; Marr, A. McA.; Rankin, D. W. H.; Schröder, M. *Acta Crystallogr., Sect. C* **1988**, *44*, 935−936.

(23) (a) Myrick, M. L.; Blakley, R. L.; DeArmond, M. K. *J. Phys. Chem.* **1989**, *93*, 3936−3940. (b) Myrick, M. L.; DeArmond, M. K. *J. Phys. Chem.* **1989**, *93*, 7099−7107.

(24) Rogers, C. W.; Patrick, B. O.; Retting, S. J.; Wolf, M. O. *J. Chem. Soc., Dalton Trans.* **2001**, 1278−1283.

(25) (a) Söderberg, B. C. G. *Coord. Chem. Rev.* **2002**, *224*, 171−243. (b) Ungváry, F. *Coord. Chem. Rev.* **2001**, *213*, 1−50. (c) Slone, C. S.; Weinberger, D. A.; Mirkin, C. A. *Prog. Inorg. Chem.* **1999**, *48*, 233−350. (d) Noyori, R.; Ohkuma, T. *Pure Appl. Chem.* **1999**, *71*, 1493−1501. (e) Jessop, P. G.; Hsiao, Y.; Ikariya, T.; Noyori, R. *J. Am. Chem. Soc.* **1996**, *118*, 344−355.

(26) (a) Zhu, Y.; Millet, D. B.; Wolf, M. O.; Rettig, S. J. *Organometallics* **1999**, *18*, 1930−1938. (b) Zhu, Y.; Wolf, M. O.; Yao, G. P. A. *Inorg. Chem.* **1997**, *36*, 5483−5487.

(27) Warren, L. F.; Bennett, M. A. *Inorg. Chem.* **1976**, *15*, 3126−3140.

(28) Lay, P. A.; Sargeson, A. M.; Taube, H. *Inorg. Synth.* **1986**, *24*, 291−299.

Chart 2. Six Possible Complexes for the Series $[Ru(bpy)_{3-n}(Me_2Pqn)_n]^{2+}$ (n = 1, 2, or 3)

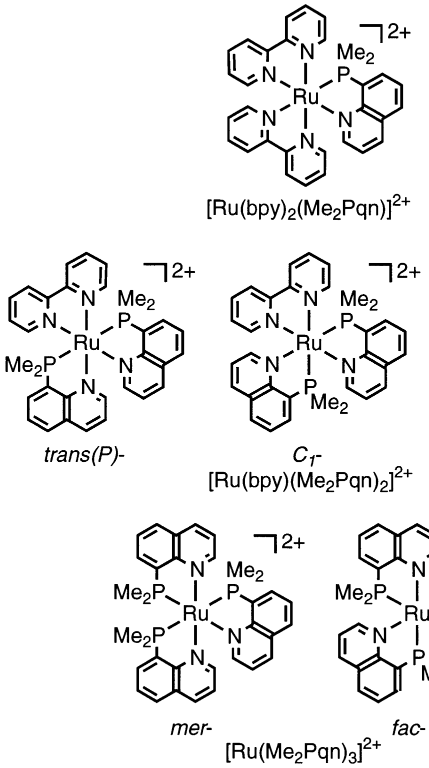

were formed. All of the solvents used in the preparation of the complexes were deaerated with argon for 20 min immediately before use.

$[Ru(bpy)_2(Me_2Pqn)](PF_6)_2$ (1). To a suspension of *cis*-$[RuCl_2(bpy)_2]\cdot 2H_2O$ (1.67 g, 3.22 mmol) in ethylene glycol (30 cm^3) was added Me$_2$Pqn (0.60 g, 3.2 mmol) dropwise with stirring. The mixture was refluxed for 1 h to give a clear orange solution, and an excess amount of aqueous NH_4PF_6 solution was added while the solution was hot. After the mixture was cooled to room temperature, the resulting orange precipitate was collected by filtration, washed with diethyl ether (30 cm^3), and dried in vacuo. The crude product was recrystallized from dichloromethane/diethyl ether, affording orange plate crystals of **1** as dichloromethane solvate. Yield: 2.43 g (85%). Anal. Found: C, 40.86; H, 3.15; N, 7.39. Calcd for $\mathbf{1}\cdot 0.5CH_2Cl_2 = C_{31.5}H_{29}ClF_{12}N_5P_3Ru$: C, 40.46; H, 3.13; N, 7.49. ^{1}H NMR (CD_3CN): δ 0.844 (d, $^2J_{P-H}$ = 9.2 Hz, 3H, PCH$_3$), 1.968 (d, $^2J_{P-H}$ = 9.2, 3H, PCH$_3$), 7.25−8.50 (m, 22H, py and qn). $^{13}C\{^1H\}$ NMR (CD_3CN): δ 9.77 (d, $^1J_{P-C}$ = 29.6 Hz, PCH$_3$), 12.53 (d, $^1J_{P-C}$ = 32.4, PCH$_3$). $^{31}P\{^1H\}$ NMR (CD_3CN): δ 39.09 (s).

$[Ru(phen)_2(Me_2Pqn)](PF_6)_2$ (1′). This complex was prepared by a method similar to that for **1** using *cis*-$[RuCl_2(phen)_2]\cdot 2H_2O$. Recrystallization from dichloromethane/methanol afforded red-brown needle crystals. Yield: 17%. Anal. Found: C, 44.39; H, 2.87; N, 7.46. Calcd for $C_{35}H_{28}F_{12}N_5P_3Ru$: C, 44.69; H, 3.00; N, 7.45. ^{1}H NMR (CD_3CN): δ 0.611 (d, $^2J_{P-H}$ = 9.6 Hz, 3H, PCH$_3$), 2.027 (d, $^2J_{P-H}$ = 9.2, 3H, PCH$_3$), 7.39−8.78 (m, 22H, phen and qn). $^{13}C\{^1H\}$ NMR (CD_3CN): δ 11.38 (d, $^1J_{P-C}$ = 30.8 Hz, PCH$_3$), 13.90 (d, $^1J_{P-C}$ = 32.3, PCH$_3$). $^{31}P\{^1H\}$ NMR (CD_3CN): δ 38.91 (s).

$[RuCl_2(bpy)(dmso)_2]$. A mixture of *cis*-$[RuCl_2(dmso)_4]$ (1.04 g, 2.15 mmol) and bpy (0.511 g, 3.27 mmol) in chloroform (50 cm^3) was refluxed for 2 h and then cooled to room temperature. A small amount of precipitate formed was filtered off, and the red-purple filtrate was evaporated to dryness under reduced pressure. The residue was extracted with acetone (150 cm^3), and the extract was concentrated (to ca. 20 cm^3) under reduced pressure. Diethyl ether (150 cm^3) was added with vigorous stirring to the concentrate to give a brown precipitate, which was collected by filtration, washed with diethyl ether (30 cm^3), and dried in vacuo. Yield: 0.898 g. This product was found to be a mixture of geometrical isomers of $[RuCl_2(bpy)(dmso)_2]$ by the elemental analysis (Anal. Found: C, 35.10: H, 4.15: N, 5.86. Calcd for $C_{14}H_{20}Cl_2N_2O_2RuS_2$: C, 34.71: H, 4.16: N, 5.78) and the ^{1}H NMR spectrum.

***trans(P)*-$[Ru(bpy)(Me_2Pqn)_2](PF_6)_2$ (*tP*-2).** The product (geometrical mixture) of $[RuCl_2(bpy)(dmso)_2]$ (1.04 g, 2.14 mmol) was suspended in ethylene glycol (20 cm^3), and Me$_2$Pqn (0.80 g, 4.2 mmol) was added dropwise with stirring. The mixture was refluxed for 3 h in the dark, and an excess amount of aqueous NH_4PF_6 solution was added while the mixture was hot. The solution was concentrated (to ca. 5 cm^3) under reduced pressure, and the resulting orange precipitate was collected by filtration, washed with diethyl ether (30 cm^3), and dried in vacuo. The crude product was recrystallized from methanol in the dark, affording orange prismatic crystals of ***tP*-2**. Yield: 1.19 g (60%). Anal. Found: C, 40.77; H, 3.61; N, 6.06. Calcd for $\mathbf{\mathit{tP}\text{-}2}\cdot H_2O = C_{32}H_{34}F_{12}N_4OP_4Ru$: C, 40.73; H, 3.63; N, 5.94. ^{1}H NMR (CD_3CN): δ 0.697 (virtual t, $^2J_{P-H}$ = 6.6 Hz, 6H, PCH$_3$), 1.803 (virtual t, $^2J_{P-H}$ = 5.7, 6H, PCH$_3$), 7.21−8.91 (m, 20H, py and qn). $^{31}P\{^1H\}$ NMR (CD_3CN): δ 20.89 (s).

***C*$_1$-$[Ru(bpy)(Me_2Pqn)_2](PF_6)_2$ (*C*$_1$-2).** An acetonitrile solution (50 cm^3) of ***tP*-2** (1.41 g, 1.52 mmol) was exposed to room light (15 W fluorescence desk lamp) at room temperature for 1 d and then evaporated to dryness under reduced pressure. The yellow residue was recrystallized from methanol, affording yellow microcrystals of ***C*$_1$-2**. Yield: 1.36 g (96%). Anal. Found: C, 41.71; H, 3.62; N, 6.00. Calcd for $C_{32}H_{32}F_{12}N_4P_4Ru$: C, 41.53; H, 3.48; N, 6.05. ^{1}H NMR (CD_3CN): δ 0.532 (d, $^2J_{P-H}$ = 8.7 Hz, 3H, PCH$_3$), 0.811 (d, $^2J_{P-H}$ = 9.4, 3H, PCH$_3$), 1.963 (d, $^2J_{P-H}$ = 9.0, 3H, PCH$_3$), 2.196 (d, $^2J_{P-H}$ = 8.2, 3H, PCH$_3$), 7.22−8.59 (m, 20H, py and qn). $^{13}C\{^1H\}$ NMR (CD_3CN): δ 11.82 (d, $^1J_{P-C}$ = 29.1 Hz, PCH$_3$), 13.74 (d, $^1J_{P-C}$ = 24.0, PCH$_3$), 14.28 (d, $^1J_{P-C}$ = 32.4, PCH$_3$), 17.36 (d, $^1J_{P-C}$ = 33.5, PCH$_3$). $^{31}P\{^1H\}$ NMR (CD_3CN): δ 35.81 (d, $^2J_{P-P}$ = 34.5 Hz), 38.46 (d).

***mer*-$[Ru(Me_2Pqn)_3](PF_6)_2$ (*m*-3).** To a suspension of *cis*-$[RuCl_2(dmso)_4]$ (0.746 g, 1.54 mmol) in ethylene glycol (20 cm^3) was added Me$_2$Pqn (0.875 g, 4.62 mmol) dropwise with stirring; the mixture was refluxed for 2 d. An excess amount of aqueous NH_4PF_6 solution was added, and the solution was filtered while hot to remove a black precipitate. The filtrate was cooled to room temperature to give a yellow precipitate, which was collected by filtration, washed with diethyl ether (30 cm^3), and dried in vacuo. The crude product was recrystallized from methanol in the dark, depositing yellow plate crystals of ***m*-3**. Yield: 0.443 g (30%). Anal. Found: C, 39.25; H, 3.72; N, 4.05. Calcd for $\mathbf{\mathit{m}\text{-}3}\cdot CH_2Cl_2 = C_{34}H_{38}Cl_2F_{12}N_3P_5Ru$: C, 39.13; H, 3.67; N, 4.03. ^{1}H NMR (CD_3CN): δ 0.864 (dd, $^2J_{P-H}$ and $^4J_{P-H}$ = 6.7 and 1.0 Hz, 3H, PCH$_3$), 1.297 (d, $^2J_{P-H}$ = 7.1, 3H, PCH$_3$), 1.362 (d, $^2J_{P-H}$ = 9.0, 3H, PCH$_3$), 1.773 (dd, $^2J_{P-H}$ and $^4J_{P-H}$ = 7.0 and 1.5, 3H, PCH$_3$), 2.027 (dd, $^2J_{P-H}$ and $^4J_{P-H}$ = 8.8 and 2.8, 3H, PCH$_3$), 2.101 (dd, $^2J_{P-H}$ and $^4J_{P-H}$ = 6.4 and 1.7, 3H, PCH$_3$), 7.19−8.90 (m, 18H, qn). $^{31}P\{^1H\}$ NMR

---

(29) (a) Alessio, A.; Mestroni, G.; Nardin, G.; Attia, W. M.; Calligaris, M.; Sava, G.; Zorzet, S. *Inorg. Chem.* **1988**, *27*, 4099−4106. (b) Evans, I. P.; Spencer, A.; Wilkinson, G. *J. Chem. Soc., Dalton Trans.* **1973**, 204−209.

(30) Crosby, G. A.; Elfring, W. H., Jr. *J. Phys. Chem.* **1976**, *80*, 2206−2211.

Table 1. Crystallographic Data for $[Ru(bpy)_2(Me_2Pqn)](PF_6)_2{\cdot}CH_2Cl_2$, *trans(P)*-$[Ru(bpy)(Me_2Pqn)_2](PF_6)_2$, *mer*-$[Ru(Me_2Pqn)_3](PF_6)_2{\cdot}CH_2Cl_2$, and *fac*-$[Ru(Me_2Pqn)_3](PF_6)_2$

	1·CH_2Cl_2	***tP*-2**	***m*-3**·CH_2Cl_2	***f*-3**
empirical formula	$C_{32}H_{30}Cl_2F_{12}N_5P_3Ru$	$C_{32}H_{32}F_{12}N_4P_4Ru$	$C_{34}H_{38}Cl_2F_{12}N_3P_5Ru$	$C_{33}H_{36}F_{12}N_3P_5Ru$
fw	977.49	925.57	1043.49	958.57
cryst color, shape	orange, plate	orange, column	yellow, plate	yellow, block
size of specimen/mm	0.27 × 0.26 × 0.10	0.41 × 0.23 × 0.12	0.40 × 0.36 × 0.10	0.45 × 0.40 × 0.30
T/°C	23	23	23	23
λ(Mo Kα)/Å	0.71073	0.71073	0.71073	0.71073
cryst syst	monoclinic	orthorhombic	triclinic	monoclinic
space group	$P2_1/c$ (No. 14)	$Fdd2$ (No. 43)	$P\bar{1}$ (No. 2)	$C2/c$ (No. 15)
a/Å	9.143(7)	37.414(8)	17.811(5)	20.843(3)
b/Å	33.977(10)	40.172(7)	18.643(7)	17.797(3)
c/Å	12.521(8)	9.987(1)	13.382(3)	23.939(3)
α/deg	90	90	98.45(3)	90
β/deg	95.54(5)	90	105.95(2)	115.644(9)
γ/deg	90	90	85.06(3)	90
V/Å^3	3846(4)	15011(4)	4221(2)	8005(2)
Z	4	16	4	8
ρ_{calcd}/Mg m^{-3}	1.688	1.638	1.642	1.591
μ(Mo Kα)/mm^{-1}	0.762	0.678	0.771	0.676
$2\theta_{max}$/deg	60	60	60	60
$R1(F^2)$ [$F^2 > 2\sigma(F^2)$]	0.059	0.039	0.063	0.065
$wR2(F^2)$ (all data)	0.207	0.119	0.246	0.248

(CD_3CN): δ 18.98 (P^a, dd, $^2J_{P^a-P^b} = 280.4$ and $^2J_{P^a-P^c} = 34.5$ Hz), 23.46 (P^b, dd, $^2J_{P^b-P^c} = 32.6$), 36.66 (P^c, virtual t).

***fac*-$[Ru(Me_2Pqn)_3](PF_6)_2$ (*f*-3).** A mixture of *cis*-$[RuCl_2(dmso)_4]$ (1.11 g, 2.30 mmol) and Me_2Pqn (0.43 g, 2.27 mmol) in chloroform (50 cm^3) was refluxed for 2 h, cooled to room temperature, and then filtered. The filtrate was concentrated (to ca. 20 cm^3) under reduced pressure, and diethyl ether (150 cm^3) was added with vigorous stirring. The deep red precipitate formed was collected by filtration, washed with diethyl ether, and dried in vacuo. Yield: 0.567 g. Anal. Found: C, 33.72: H, 4.79: N, 2.62. Calcd for $RuCl_2(Me_2Pqn)(dmso)(H_2O) = C_{13}H_{20}Cl_2NO_2RuPS$: C, 34.06: H, 4.40: N, 3.06. The product obtained above (0.376 g, 0.822 mmol) was suspended in ethylene glycol (20 cm^3), and Me_2Pqn (0.32 g, 1.7 mmol) was added dropwise with stirring. The mixture was refluxed for 2 d, and an excess amount of aqueous NH_4PF_6 was added while the mixture was hot. The solution was cooled to room temperature to give a yellow precipitate, which was collected by filtration, washed with diethyl ether (30 cm^3), and dried in vacuo. The crude product was recrystallized from acetonitrile/methanol, affording pale yellow plate crystals of ***f*-3**. Yield: 0.671 g (78%). Anal. Found: C, 40.98; H, 3.59; N, 4.33. Calcd for $C_{33}H_{36}F_{12}N_3P_5Ru$: C, 41.35; H, 3.79; N, 4.38. ^1H NMR (CD_3CN): δ 0.675 (filled-in d, $^2J_{P-H} = 9.1$ Hz, 9H, PCH_3), 2.016 (filled-in d, $^2J_{P-H} = 8.0$, 9H, PCH_3), 7.38−8.66 (m, 18H, qn). $^{13}C\{^1H\}$ NMR (CD_3CN): δ 13.79 (d, $^1J_{P-C} = 31.3$ Hz, PCH_3), 18.52 (d, $^1J_{P-C} = 54.2$, PCH_3). $^{31}P\{^1H\}$ NMR (CD_3CN): δ 37.59 (s).

$[Ru(bpy)_2(dmpb)](PF_6)_2$ (4). This complex was prepared by a method similar to that for complex **1** in 48% yield. Anal. Found: C, 39.62; H, 3.41; N, 6.30. Calcd for $C_{30}H_{32}F_{12}N_4P_4Ru$: C, 39.97; H, 3.58; N, 6.21. ^1H NMR (CD_3CN): δ 0.759 (filled-in d, $^2J_{P-H} = 9.2$ Hz, 6H, PCH_3), 1.750 (filled-in d, $^2J_{P-H} = 9.2$, 6H, PCH_3), 7.38−8.48 (m, 20H, py and phen). $^{13}C\{^1H\}$ NMR (CD_3CN): δ 12.68 (d, $^1J_{P-C} = 17.3$ Hz, PCH_3), 13.11 (d, $^1J_{P-C} = 13.4$, PCH_3). $^{31}P\{^1H\}$ NMR (CD_3CN): δ 46.41 (s).

Crystallography. The X-ray intensities were measured at 23 °C on a Rigaku automated four-circle diffractometer, AFC-5R or AFC-7R, equipped with graphite-monochromated Mo Kα radiation (λ = 0.71073 Å). Absorption corrections were made either by the numerical integration method[31a] or by an empirical method based on three sets of Ψ-scan data.[31b] The structures were solved by the direct method using the SHELXS-86 program[32a] and refined on F^2 by full-matrix least-squares using SHELXL-97.[32b] All non-hydrogen atoms were refined anisotropically, and all H atoms were treated as riding models. All calculations were carried out using the TeXsan software package.[33] The crystallographic data are summarized in Table 1.

Measurements. The ^1H, $^{13}C\{^1H\}$, and $^{31}P\{^1H\}$ NMR spectra were recorded at 30 °C on a JEOL EX-270 or GSX-400 spectrometer using tetramethylsilane as an internal reference for ^1H and $^{13}C\{^1H\}$ and 85% H_3PO_4 as an external reference for $^{31}P\{^1H\}$. UV−vis absorption spectra were obtained on a Perkin-Elmer Lambda19 spectrophotometer at room temperature. Cyclic voltammograms were measured at 25 °C on a BAS CV-27 electrochemical analyzer at a scan rate of 200 mV s^{-1} in acetonitrile solutions ([complex] = 2.0×10^{-3} mol dm^{-3}; 0.1 mol dm^{-3} Bu_4NBF_4). A glassy carbon disk, a platinum wire, and a Ag/Ag$^+$ electrode (Ag/0.01 mol dm^{-3} $AgNO_3$) were used as the working, auxiliary, and reference electrodes, respectively. The redox potentials of the samples were calibrated by the redox signal for the ferrocene/ferrocenium couple, which was observed at +0.42 V vs Ag/Ag$^+$. Luminescence spectra in EtOH/MeOH (4:1) glass were recorded on a Shimadzu RF-5300 PC spectrophotofluorometer equipped with a liquid nitrogen dewar. Emission decays were measured with a fluorescence lifetime measurement system, Hamamatsu C4780, which is constructed with a N_2 laser, a spectrogram, and a streak camera. The temperature control was performed using a continuous-flow cryostat, Oxford Optistat DN.

Results and Discussion

Preparation and Characterization of Me_2Pqn Complexes. A reaction of *cis*-$[RuCl_2(bpy)_2]{\cdot}2H_2O$ and Me_2Pqn in refluxing ethylene glycol, followed by the addition of aqueous NH_4PF_6, afforded an orange product of **1** in 85% yield. The analogous phen complex **1′** was prepared similarly in moderate yield. The $^{31}P\{^1H\}$ NMR spectrum of each

---

(31) (a) Coppens, P.; Leiserowitz, L.; Ravinovich, D. *Acta Crystallogr.* **1965**, *18*, 1035−1038. (b) North, A. C. T.; Phillips, D. C.; Mathews, F. S. *Acta Crystallogr., Sect. A* **1968**, *24*, 351−359.

(32) (a) Sheldrich, G. M. *Acta Crystallogr., Sect. A* **1990**, *46*, 467−473. (b) Sheldrich, G. M. *SHELXL97*; University of Göttingen: Göttingen, Germany, 1997.

(33) *TeXsan: Single-Crystal Structure Analysis Software*, ver. 1.11; Molecular Structure Corp.: The Woodlands, TX; Rigaku Co. Ltd.: Akishima, Tokyo, Japan, 2000.

product in CD_3CN gave a single resonance, and the ^1H NMR spectrum showed two doublet resonances for PCH_3 (see the Experimental Section), indicating the chelate coordination of Me_2Pqn to the Ru(bpy or phen)$_2$ center.

As a starting material for **2**, $[RuCl_2(bpy)(dmso)_2]$ was prepared by a method similar to that for $[RuCl_2(dmbpy)(dmso)_2]$ (dmbpy = 4,4′-dimethyl-2,2′-bipyridine).[16c] The elemental analysis of the product confirmed that it had a composition of $RuCl_2(bpy)(dmso)_2$, and the ^1H NMR spectrum indicated that it was a mixture of some geometrical and linkage (dmso-κO and dmso-κS) isomers. Since an attempt to separate these isomers was not successful, the mixture was used as was for the preparation of complex **2**. A reaction of $[RuCl_2(bpy)(dmso)_2]$ and two equimolar amounts of Me_2Pqn in refluxing ethylene glycol in the dark, followed by the addition of aqueous NH_4PF_6, gave an orange product. NMR spectroscopy confirmed the *trans(P)* geometrical structure of the product ***tP*-2**.

When the acetonitrile solution of ***tP*-2** was exposed to room light for 1 d, it was found that the complex isomerized completely to ***C*$_1$-2**. The NMR spectral data of the product by photolysis indicated that the $[Ru(bpy)(Me_2Pqn)_2]^{2+}$ moiety was in C_1 symmetry. The photochemical conversion from *trans(P)*- to C_1-isomers occurred quantitatively in acetonitrile within several hours by irradiation of light corresponding to the MLCT transition (413 nm) of ***tP*-2**. Solvent dependence was observed for this photoisomerization reaction; it took place with a moderate rate in acetonitrile, dichloromethane, acetone, *N,N*-dimethylformamide, and water, while the isomerization was undetectably slow in methanol, ethanol, and dimethyl sulfoxide.

The C_1-isomer was thermally reconverted to the original *trans(P)*-isomer, when a solution of ***C*$_1$-2** in ethylene glycol was heated to reflux in the dark for several hours. Therefore, the free energy barrier between C_1- and *trans(P)*-isomers is rather high, and both of these species are stable at room temperature; thermodynamically the more stable geometrical isomer in the ground state is the *trans(P)*-isomer. Geometrical isomers with such a photo- and thermoinduced structural interconversion have been demonstrated for *cis*- and *trans*-$[Ru(ROCS_2)_2(PPh_3)_2]^{0/+}$ (R = alkyl or benzyl),[34] and in the xantate complexes the stabilities depend on the oxidation state of ruthenium; Ru^{II} prefers the *cis*-isomer, while Ru^{III} stabilizes the *trans*-isomer. In the present complexes, however, both isomers exhibit reversible $Ru^{III/II}$ redox signals in the cyclic voltammograms (vide infra). Therefore, it seems that the nature of the ligands determines the geometrical preference of the photoconverted isomers.

It was not possible to isolate the *trans(N)*-isomer of **2** (Chart 2); when $[RuCl_2(bpy)(dmso)_2]$ and two equimolar amounts of Me_2Pqn were refluxed in ethylene glycol with exposure to room light, a mixture of *trans(P)*- and C_1-isomers was obtained together with uncharacterizable byproducts that may contain some *trans(N)*-isomer. However, an attempt to isolate the *trans(N)*-isomer by column chromatography or fractional recrystallization was not successful.

A reaction of *cis*-$[RuCl_2(dmso)_4]$ with three equimolar amounts of Me_2Pqn in refluxing ethylene glycol, followed by the addition of aqueous NH_4PF_6, yielded a yellow precipitate with the composition of $Ru(Me_2Pqn)_3(PF_6)_2$. Due to the partial reduction of ruthenium(II) to ruthenium black during this reaction, the yield of the complex was relatively low (~30%). The $^{31}P\{^1H\}$ NMR spectrum of the product gave two doublet-of-doublet signals at δ 18.98 and 23.46 and a virtual triplet signal at δ 36.66 with coupling constants of $^2J_{P-P}$ = 280.4, 34.5, and 32.6 Hz. In the ^1H NMR spectrum, we observed six different sets of resonances for PCH_3, two doublets and four doublets-of-doublets (see the Experimental section). These NMR data correspond to $[Ru(Me_2Pqn)_3](PF_6)_2$ in C_1 symmetry (***m*-3**).

We examined another synthetic procedure for complex **3** via the isolation of the intermediate mono(Me_2Pqn) complex. A reaction of *cis*-$[RuCl_2(dmso)_4]$ and an equimolar amount of Me_2Pqn in chloroform gave a deep red product with the composition $RuCl_2(Me_2Pqn)(dmso)(H_2O)$. As this compound decomposed rather rapidly in solution, it was not possible to characterize the structure of this product. Therefore, we used this product as was for the further reaction with two equimolar amounts of Me_2Pqn in refluxing ethylene glycol. Such a reaction produced pale yellow plate crystals in 60% yield (based on *cis*-$[RuCl_2(dmso)_4]$) by the addition of aqueous NH_4PF_6, followed by recrystallization from an acetonitrile/methanol mixture. In contrast to the spectra of ***m*-3**, the $^{31}P\{^1H\}$ NMR spectrum of this pale yellow product exhibited only one singlet signal at δ 37.59, and in the ^1H NMR spectrum there were only two filled-in doublet resonances for PCH_3. Such NMR evidence strongly indicates that the product is the *fac*-isomer ***f*-3**. This isomer was also obtained quantitatively from ***m*-3** by photochemical reaction in acetonitrile, dichloromethane, acetone, *N,N*-dimethylformamide, methanol, or dimethyl sulfoxide by irradiation of light that corresponds to the MLCT band of ***m*-3** (385 nm). Furthermore, the thermal reconversion to ***m*-3** was also achieved by refluxing ***f*-3** in ethylene glycol.

Crystal Structures. The crystal structures of **1**·CH_2Cl_2, ***tP*-2**, ***m*-3**·CH_2Cl_2, and ***f*-3** were determined by X-ray analyses. Complex ***m*-3** crystallized, together with one dichloromethane molecule, in triclinic space group $P\bar{1}$ with $Z = 4$; in an asymmetric unit there are two independent complex cations whose molecular structures are similar to each other. The molecular structures of the complex cations in **1**·CH_2Cl_2, ***tP*-2**, ***m*-3**·CH_2Cl_2, and ***f*-3** are shown in Figures 1−4, respectively. The Me_2Pqn ligand coordinates to the Ru^{II} ion via P and N donor atoms to form a five-membered chelate ring.

The complex cation in ***f*-3** is approximately in C_3 molecular symmetry; no remarkable distortion as a result of the intramolecular steric interaction was observed. The average Ru−P and Ru−N bond lengths are 2.258(1) and 2.186(4) Å, respectively.

The Ru−P bond length in **1**·CH_2Cl_2 (Ru−P(1) = 2.260(2) Å) coincides well with those in ***f*-3**, while the Ru−N(qn) bond length in **1**·CH_2Cl_2 (Ru−N(1) = 2.130(5) Å) is much shorter than those in ***f*-3**, indicating a strong *trans* influence

---

[34] Bag, N.; Lahiri, G. K.; Chakravorty, A. *J. Chem. Soc., Dalton Trans.* **1990**, 1557−1561.

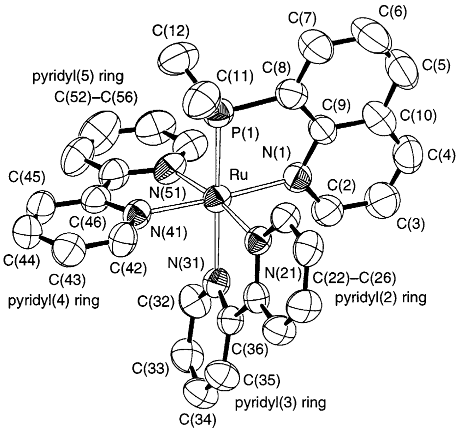

Figure 1. Perspective drawing (50% probability level) of the cationic complex in **1**·CH_2Cl_2. Selected distances (Å) and angles (deg): Ru−P(1) = 2.260(2), Ru−N(1) = 2.109(5), Ru−N(21) = 2.086(5), Ru−N(31) = 2.130(5), Ru−N(41) = 2.052(5), Ru−N(51) = 2.066(5); P(1)−Ru−N(1) = 83.6(2), P(1)−Ru−N(31) = 175.9(1), N(21)−Ru−N(31) = 77.6(2), N(41)−Ru−N(51) = 78.1(2). Hydrogen atoms are omitted for clarity.

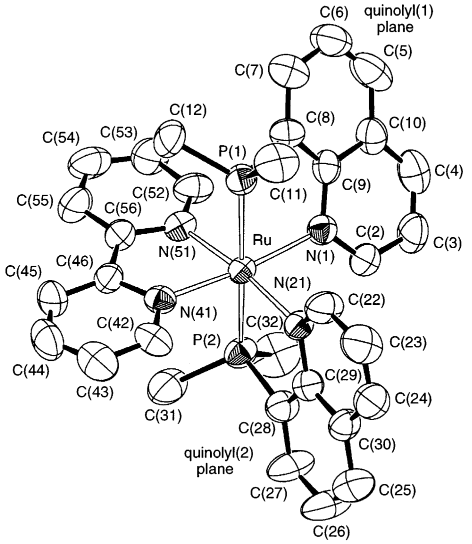

Figure 2. Perspective drawing (50% probability level) of the cationic complex in ***tP*-2**. Selected distances (Å) and angles (deg): Ru−P(1) = 2.359(2), Ru−P(2) = 2.326(2), Ru−N(1) = 2.127(5), Ru−N(21) = 2.119(5), Ru−N(41) = 2.063(5), Ru−N(51) = 2.078(5); P(1)−Ru−N(1) = 80.5(2), P(2)−Ru−N(21) = 82.5(1), N(41)−Ru−N(51) = 78.8(2), P(1)−Ru−P(2) = 174.70(7), N(1)−Ru−N(21) = 88.1(2). Hydrogen atoms are omitted for clarity.

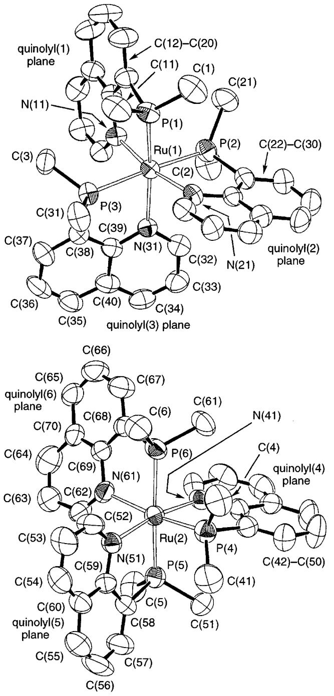

Figure 3. Perspective drawings (50% probability level) of the two crystallographically independent cationic complexes in ***m*-3**·CH_2Cl_2. Selected distances (Å) and angles (deg): Ru(1)−P(1) = 2.247(2), Ru(1)−P(2) = 2.321(2), Ru(1)−P(3) = 2.365(2), Ru(1)−N(11) = 2.103(5), Ru(1)−N(21) = 2.118(6), Ru(1)−N(31) = 2.232(5), Ru(2)−P(4) = 2.272(2), Ru(2)−P(5) = 2.330(2), Ru(2)−P(6) = 2.382(2), Ru(2)−N(41) = 2.112(6), Ru(2)−N(51) = 2.128(6), Ru(2)−N(61) = 2.213(6); P(1)−Ru(1)−N(11) = 83.7(2), P(2)−Ru(1)−N(21) = 82.4(2), P(3)−Ru(1)−N(31) = 79.3(2), P(4)−Ru(2)−N(41) = 84.3(2), P(5)−Ru(2)−N(51) = 82.1(2), P(6)−Ru(2)−N(61) = 80.1(2). Hydrogen atoms are omitted for clarity.

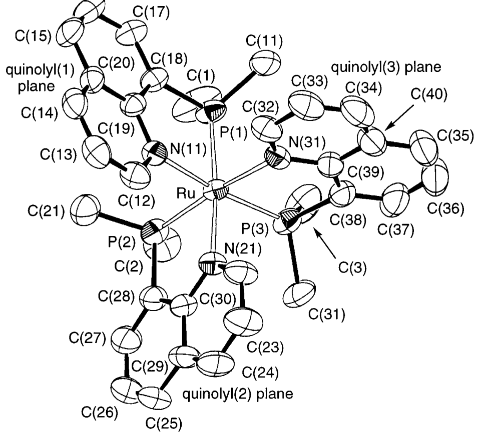

Figure 4. Perspective drawing (50% probability level) of the cationic complex in ***f*-3**. Selected distances (Å) and angles (deg): Ru−P(1) = 2.259(1), Ru−P(2) = 2.262(1), Ru−P(3) = 2.252(1), Ru−N(11) = 2.178(4), Ru−N(21) = 2.180(4), Ru−N(31) = 2.201(4); P(1)−Ru−N(11) = 82.1(1), P(2)−Ru−N(21) = 82.5(1), P(3)−Ru−N(31) = 82.6(1). Hydrogen atoms are omitted for clarity.

of the Me_2P- donor group. The strong *trans* influence of the Me_2P- group also affects the Ru−N(bpy) bond lengths in **1**·CH_2Cl_2; the Ru−N(31) bond *trans* to the Me_2P- donor is longer by ca. 0.06 Å than the other Ru−N(bpy) bonds in **1**·CH_2Cl_2 (average 2.068 Å) and the Ru−N bonds in $[Ru(bpy)_3](PF_6)_2$ (2.056 Å).[35] While the rings in one of the bpy ligands (pyridyl(4) and pyridyl(5) rings; see Figure 1) are nearly coplanar to each other (the dihedral angle between them is 2.1(2)°) and to the coordination plane defined by Ru, N(41), and N(51), the coordination geometry of the other bpy exhibited distortion from planarity (Table 2). The pyridyl(2) and pyridyl(3) rings have dihedral angles of 10.2(2)° and 13.3(2)°, respectively, to the coordination plane defined by Ru, N(21), and N(31), and the dihedral angle between these two planes is 7.8(2)°. Such a distortion in the coordination geometry of bpy seems to appear as a result of the intramolecular steric repulsion between the $C(11)H_3$ moiety of Me_2Pqn and the C(22)H of the pyridyl(2) plane. A similar but slightly larger distortion of the bpy coordination geometry was reported for the corresponding Ph_2Pqn complex $[Ru(bpy)_2(Ph_2Pqn)](PF_6)_2$.[36]

---

[35] Rillema, P.; Jones, D. S.; Levy, H. A. *J. Chem. Soc., Chem. Commun.* **1979**, 849−851.

Table 2. Dihedral Angles (ϕ/deg) between the Ru$^{\mathrm{II}}$ Coordination Plane and the Least-Squared Quinolyl or Pyridyl Ring in the Me$_2$Pqn Complexes[a]

1·CH$_2$Cl$_2$	
plane{Ru,P(1),N(1)} vs plane quinolyl(1)	10.5(1)
plane{Ru,N(21),N(31)} vs plane pyridyl(2)	10.2(2)
plane{Ru,N(21),N(31)} vs plane pyridyl(3)	13.3(2)
plane{Ru,N(41),N(51)} vs plane pyridyl(4)	0.8(2)
plane{Ru,N(41),N(51)} vs plane pyridyl(5)	1.4(2)
_tP_-2	
plane{Ru,P(1),N(1)} vs plane quinolyl(1)	24.2(1)
plane{Ru,P(2),N(2)} vs plane quinolyl(2)	4.4(1)
plane{Ru,N(41),N(51)} vs plane pyridyl(4)	4.1(2)
plane{Ru,N(41),N(51)} vs plane pyridyl(5)	5.1(2)
_m_-3·CH$_2$Cl$_2$	
plane{Ru(1),P(1),N(11)} vs plane quinolyl(1)	9.8(1)
plane{Ru(1),P(2),N(21)} vs plane quinolyl(2)	9.8(2)
plane{Ru(1),P(3),N(31)} vs plane quinolyl(3)	15.4(1)
plane{Ru(2),P(4),N(41)} vs plane quinolyl(4)	8.9(1)
plane{Ru(2),P(5),N(51)} vs plane quinolyl(5)	9.3(1)
plane{Ru(2),P(6),N(61)} vs plane quinolyl(6)	16.2(1)
_f_-3	
plane{Ru,P(1),N(11)} vs plane quinolyl(1)	7.84(7)
plane{Ru,P(2),N(21)} vs plane quinolyl(2)	8.1(1)
plane{Ru,P(3),N(31)} vs plane quinolyl(3)	4.3(1)

[a] For a definition of the quinolyl and pyridyl planes, see Figures 1−4.

Table 3. Cyclic Voltammetry Results of the Ruthenium(II) Complexes[a]

	oxidation	reduction		
complex	$E_{1/2}$(Ru$^{\mathrm{III/II}}$)	$E_{1/2}$(red 1)	$E_{1/2}$(red 2)	$\Delta E_{1/2}$[b]
[Ru(bpy)$_3$](PF$_6$)$_2$	+1.06	−1.55	−1.75	21.05
[Ru(bpy)$_2$(phen)](PF$_6$)$_2$	+1.08	−1.54	−1.71	21.13
1	+1.11	−1.47	−1.73	20.81
_tP_-2	+1.19	−1.56[c]	−1.74[c]	
_C_$_1$-2	+1.33	−1.48	−1.69	22.67
_m_-3	+1.23	−1.56[c]	−1.72[c]	
_f_-3	+1.59	−1.48	−1.61	24.76
4	+1.35	−1.52	−1.72	23.15

[a] Potentials are in volts vs SCE. [b] The difference between the oxidation and the first reduction potentials on a 10^3 cm^{-1} scale. [c] The redox couple was irriversible; only the cathodic peak positions (E_{pc}) are listed.

The Ru−P bonds in **_tP_-2** (Ru−P(1) = 2.358(2) Å, Ru−P(2) = 2.326(2) Å) are considerably longer than those in **1** and **_f_-3**, indicating that the strong *trans* influence of the Me$_2$P− group in Me$_2$Pqn mutually elongates the *trans* Ru−P bonds. In complex **_tP_-2**, the coordination geometry of two Me$_2$Pqn ligands is markedly inequivalent; the quinolyl(2) plane composed of N(21) and C(22)−C(30) is almost coplanar to the coordination plane defined by Ru, P(2), and N(21), while the quinolyl(1) plane is largely twisted from the plane defined by Ru, P(1), and N(1). The dihedral angles between the quinolyl and the coordination planes are 4.4(1)° and 24.2(1)° for quinolyl(2) and quinolyl(1), respectively. An octahedral *trans(P)*-bis(Me$_2$Pqn) complex with planar five-membered Me$_2$Pqn ligands is expected to exhibit severe intramolecular steric interactions arising from one P−CH$_3$ group and the quinolyl ring on the other Me$_2$Pqn. However, the observed inequivalent coordination geometries of two Me$_2$Pqn ligands effectively reduces such steric congestions. A relatively large (more than 0.03 Å) difference between two Ru−P bond lengths in **_tP_-2** may be attributed to this distortion.

In the structure of **_m_-3**·CH$_2$Cl$_2$, a similar distortion of one of the Me$_2$Pqn ligands and the related difference in the Ru−P bond lengths were also observed. The dihedral angles of the quinolyl(3) and quinolyl(6) planes to the corresponding coordination planes are 15.4(1)° and 16.2(1)°, respectively, while the other quinolyl planes have a dihedral angle of less than 10° (Table 2). The Ru(1)−P(3) and Ru(2)−P(6) bonds are longer by more than 0.04 Å compared with the Ru(1)−P(2) and Ru(2)−P(5) bonds, respectively, although these mutually *trans* Ru−P bonds are still longer than the Ru(1)−P(1) and Ru(2)−P(4) bonds due to the strong *trans* influence of the Me$_2$P− group. Such a strong *trans* influence of the Me$_2$P− group induces the deviation of the Ru−N(qn) bond lengths. In fact, the Ru(1)−N(31) and Ru(1)−N(61) bonds which are *trans* to the Ru−P bonds are remarkably longer (by ca. 0.1 Å) than the mutually *trans* Ru(1)−N(11), Ru(1)−N(21), Ru(2)−N(41), and Ru(2)−N(51) bonds; these bond lengths are comparable to the Ru−N(qn) bond length in **_tP_-2**.

Electrochemistry. The cyclic voltammetry (CV) signals of the solutions containing the Me$_2$Pqn complexes, [Ru(bpy)$_3$](PF$_6$)$_2$, and [Ru(bpy)$_2$(phen)](PF$_6$)$_2$ were reversible for the Ru$^{\mathrm{III/II}}$ couple (Table 3). Moreover, the complexes, except for **_tP_-2** and **_m_-3**, exhibited two or three reversible signals at the negative potential region. The latter signals in the negative potential region were assigned to the ligand-based reduction processes.[8,9] The first reduction took place at almost identical potentials for all Me$_2$Pqn complexes **1**, **1′**, **_C_$_1$-2**, and **_f_-3** (−1.48 V vs SCE), while the corresponding signals for [Ru(bpy)$_3$](PF$_6$)$_2$ and [Ru(bpy)$_2$(phen)](PF$_6$)$_2$ appeared at a slightly more negative region (−1.55 V vs SCE).

The **_tP_-2** and **_m_-3** complexes exhibited two irreversible reduction signals with only cathodic peaks (E_{pc}) at −1.56 and −1.73 V vs SCE. As described above, photochemical isomerizations to **_C_$_1$-2** and **_f_-3**, respectively, were observed for these complexes. Therefore, the reduced complexes *trans-(P)*-[Ru(bpy)(Me$_2$Pqn)$_2$]$^{(+\text{ or }0)}$ and *mer*-[Ru(Me$_2$Pqn)$_3$]$^{(+\text{ or }0)}$ may be labile, as indicated by the extremely long Ru−P bonds in the parent complexes **_tP_-2** and **_m_-3** due to the mutual *trans* influence of the Me$_2$P− group in Me$_2$Pqn.

The redox potential of the Ru$^{\mathrm{III/II}}$ couple became more positive with increasing number of coordinated Me$_2$Pqn ligands. Therefore, the analysis on the basis of Bursten's method[37] seems applicable to the series of complexes [Ru(bpy)$_3$](PF$_6$)$_2$, **1**, **_C_$_1$-2**, and **_f_-3**:

$$E_{1/2}(\mathrm{Ru^{III/II}}) = A + Bn + Cx_{\mathrm{HOMO}}$$

where n and x_{HOMO} denote the number of coordinated Me$_2$P− donor groups and the number of Me$_2$P− π-orbitals with which the highest energy Ru$^{\mathrm{II}}$ dπ orbital interacts, respectively. Assuming that the σ-basicity and π-acidity of bpy and the quinoline moiety are identical to each other,[9,37a] the

---

(36) Suzuki, T.; Kuchiyama. T.; Kishi, S.; Kaizaki, S.; Kato, M. *Bull. Chem. Soc. Jpn.* **2002**, *75*, 2433−2439.

(37) (a) Lever, A. B. P.; Dodsworth, E. S. In *Inorganic Electronic Structure and Spectroscopy*; Solomon, E. I., Lever, A. B. P., Eds.; John Wiley & Sons: New York, 1999; Vol. II, Chapter 4. (b) Bursten, B. E.; Green, M. R. *Prog. Inorg. Chem.* **1988**, *36*, 393−485.

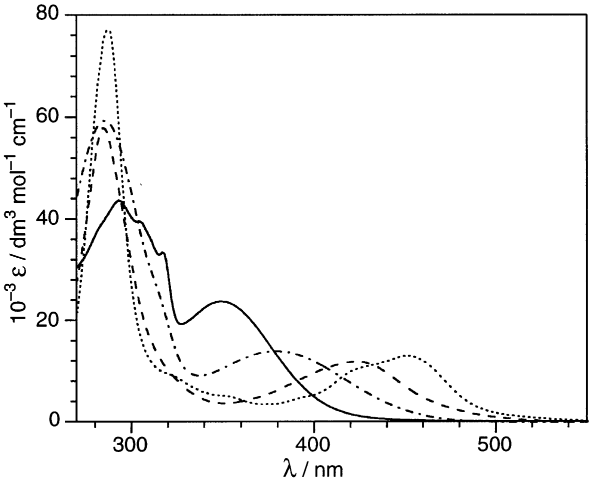

Figure 5. UV−vis absorption spectra of complex **1** (---), complex ***C***$_1$**-2** (-·-), complex ***f*-3** (—), and [Ru(bpy)$_3$](PF$_6$)$_2$ (···) in acetonitrile at room temperature.

B and *C* parameters were estimated from the observed oxidation potentials for the series of complexes as ∼0.05 and ∼0.19 V, respectively. This result indicates that the π-acidity of the Me$_2$P− group is remarkably larger than that of bpy or qn, while the difference in the electrostatic effect among Me$_2$Pqn, bpy, and qn is marginal. On the other hand, complex ***m*-3** exhibited a much lower redox potential than the calculated value ($E_{1/2}$(Ru$^{III/II}$)$_{calcd}$ ≈ +1.40 V), although the observed oxidation potential of complex ***tP*-2** was consistent with the estimated value from Bursten's equation with $B = 0.05$ V. Such a discrepancy may originate from the limitation of the parametric approach such as Bursten's method; the observed metal-centered redox potential represents not only the HOMO level of the Ru^{II} species but also the difference in the solvation energies of the Ru^{II} and Ru^{III} species in solution. The *trans(P)*-complex ***tP*-2**, with less dipole moment compared with the *mer*-complex ***m*-3**, experiences a smaller change in solvation free energy in polar solvents, and therefore, the oxidation potential is rather well described by Bursten's equation, while the redox potential for ***m*-3** is overestimated. As a result, the differences found in the crystal structures (i.e., the elongation of the mutually *trans* Ru−P bonds and the steric strain of the planar Me$_2$Pqn chelates) do not seem to affect the oxidation potential of ***tP*-2**, while the oxidation potential is lowered significantly for ***m*-3**.

UV−Vis Absorption Spectra. The UV−vis absorption spectra of a series of complexes, [Ru(bpy)$_3$](PF$_6$)$_2$, **1**, ***C***$_1$**-2**, and ***f*-3**, are shown in Figure 5, and the spectral data are listed in Table 4. Complex **1** exhibits two intense absorption bands at 423 and 288 nm. The former band with broad shoulders at the higher energy side can be assigned to the MLCT transition, and the transition energy is higher by 1500 cm^{-1} than that of [Ru(bpy)$_3$](PF$_6$)$_2$.[10,38] The higher energy absorption band centered at 288 nm is due to the bpy-based intraligand π−π* transition, since [Ru(bpy)$_3$](PF$_6$)$_2$ exhibits a similarly intense band at the same energy.[10] The analogous bis(phen) complex **1′** showed the corresponding intramolecular phen-based π−π* transition band at the higher energy region (262 nm), and this band was accompanied by a distinct lower energy shoulder. The Gaussian curve fitting revealed that there is an absorption band centered at 285 nm, which may be assigned to the quinoline-based π−π* transition. Complex ***C***$_1$**-2** exhibited spectral characteristics similar to those of complex **1**; the MLCT transition band blue-shifted to 379 nm, and the bpy-based intraligand π−π* transition band was observed at 285 nm with a broad shoulder at the lower energy side. In the spectrum of complex ***f*-3**, the quinoline-based intraligand π−π* transitions were observed as at least three sharp bands centered at 293, 310, and 318 nm, all of which are lower in energy than the bpy-based π−π* transition of [Ru(bpy)$_3$](PF$_6$)$_2$. The MLCT transition band of ***f*-3** was observed at 349 nm.

Table 4. Absorption Spectral Data[a] [λ_{max}/nm (ϵ/10^3 dm^3 mol^{-1} cm^{-1})] of the Ruthenium(II) Complexes

complex	λ_{max}(MLCT)	λ_{max}(π−π*)
[Ru(bpy)$_3$](PF$_6$)$_2$	452 (13.2), 410 (7.48)[b]	287 (77.2)
1	423 (12.0)	288 (54.6)
1′	415 (13.0), 364 (4.07)[b]	285 (25.4),[b] 262 (69.4)
***tP*-2**	410 (16.1)	315 (21.7),[b] 282 (81.3)
C$_1$**-2**	379 (14.1)	316 (23.8),[b] 285 (62.9)
***m*-3**	409 (8.22), 373 (5.85)[b]	324 (15.1),[b] 294 (17.9)
***f*-3**	349 (23.8)	318 (33.2), 310 (36.3), 293 (43.7)
4	389 (10.6)	318 (14.7),[b] 295 (20.7),[b] 281 (31.9)

[a] In acetonitrile at room temperature. [b] Absorption shoulder.

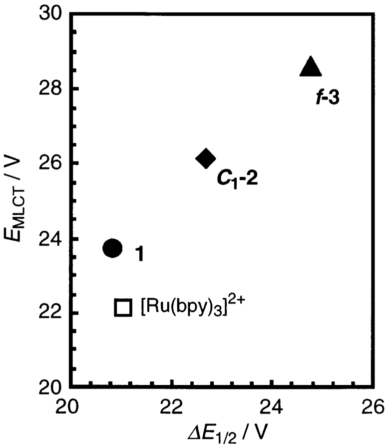

Figure 6. Potential difference between the Ru-centered oxidation and the first ligand-based reduction couples, $\Delta E_{1/2} = E_{1/2}$(Ru$^{III/II}$) − $E_{1/2}$(red1), versus the observed MLCT transition energy, E_{MLCT}, for complexes [Ru(bpy)$_3$](PF$_6$)$_2$ (□), **1** (●), ***C***$_1$**-2** (◆), and ***f*-3** (▲).

It has been well established for ruthenium(II) polypyridine complexes that the energy of the MLCT manifold increases linearly with increasing difference between the Ru-centered redox potential ($E_{1/2}$(Ru$^{III/II}$)) and the first ligand-based reduction potential ($E_{1/2}$(red1)), $\Delta E_{1/2} = E_{1/2}$(Ru$^{III/II}$) − $E_{1/2}$(red1).[9] For complexes **1**, ***C***$_1$**-2**, and ***f*-3**, an excellent linear relationship between the MLCT energy (E_{MLCT}) and $\Delta E_{1/2}$ was observed, while the plot for [Ru(bpy)$_3$](PF$_6$)$_2$ largely deviated from this relation, as shown in Figure 6. Since the changes in the Ru-centered redox potentials for the series of complexes are reasonably explained by the electrostatic and π-back-bonding effects of the Me$_2$P− donor, the anomaly observed for [Ru(bpy)$_3$](PF$_6$)$_2$ may be attributed to

---

(38) Felix, F.; Ferguson, J.; Güdel, H. U.; Ludi, A. *J. Am. Chem. Soc.* **1980**, *102*, 4096−4102.

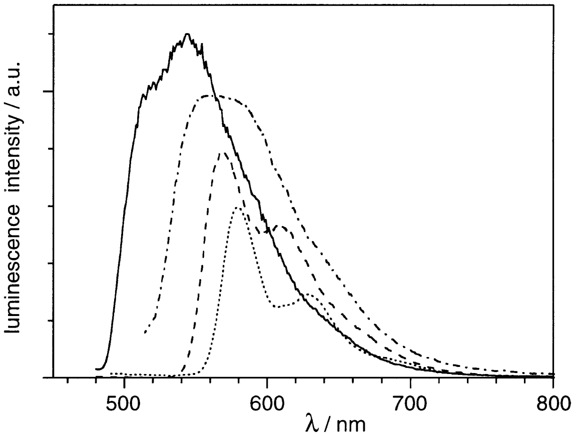

Figure 7. Emission spectra of complex **1** (---), complex ***C*$_1$-2** (-·-), complex ***f*-3** (—), and [Ru(bpy)$_3$](PF$_6$)$_2$ (···) in EtOH/MeOH (4:1) glass at 77 K. The emission intensities have been arbitrarily scaled for the sake of easier comparison. The excitation wavelength is 434 nm for complex **1**, 382 nm for complex ***C*$_1$-2**, 352 nm for complex ***f*-3**, and 457 nm for [Ru(bpy)$_3$](PF$_6$)$_2$.

a ligand-based reduction process, the difference between bpy-centered reduction for [Ru(bpy)$_3$](PF$_6$)$_2$ and the quinoline-centered reduction for the Me$_2$Pqn complexes.

As complexes ***tP*-2** and ***m*-3** did not exhibit reversible reduction signals, it was not possible to determine the unambiguous $\Delta E_{1/2}$ values for these complexes. However, it seems obvious that the low-energy MLCT transition energies of these complexes are related to the observed redox potentials, $E_{1/2}$(Ru$^{III/II}$), as the MLCT bands (Table 4) as well as the oxidation potentials (Table 3) of these complexes were observed at the positions between those for complexes **1** and ***C*$_1$-2**.

Luminescence Spectra. The photophysical properties of [Ru(bpy)$_3$](PF$_6$)$_2$ and related complexes have been intensively investigated.[8,10,39] The result obtained by the measurement of the luminescence of [Ru(bpy)$_3$](PF$_6$)$_2$ in EtOH/MeOH (4:1) frozen glass at 77 K is shown in Figure 7, emission at λ_{max}^{em} = 579 nm with a vibrational progression of $\Delta\nu$ = 1350 cm^{-1} and an emission lifetime of τ = 4.1 μs (Figure 8). This emission has been assigned to that from an ^{3}MLCT excited state.[39]

Complex ***f*-3** exhibited an intense broad emission manifold with a pronounced shoulder at the *higher* energy side; the emission maximum was observed at 536 nm and the shoulder at 501 nm (Figure 7). The emission spectrum was independent of the excitation wavelengths; the excitation with light corresponding to the MLCT band and the quinoline-based $\pi-\pi^*$ transition gave the same emission spectrum. Moreover, the excitation spectrum obtained by monitoring the intensities of the emissions at 536 and 501 nm was found to be identical to the absorption spectrum. The emissions at 536 and 501 nm were found to have a considerably long lifetime (τ = 920 μs at 77 K) compared with the lifetime of the emission of [Ru(bpy)$_3$](PF$_6$)$_2$ (Figure 8). Such a long-lived emission has rarely been observed for the ruthenium(II) polypyridine complexes, except for [Ru(*i*-bqn)$_3$](PF$_6$)$_2$ (*i*-bqn = 2,2′-biisoquinoline; τ = 96 μs in propionitrile/butyronitrile (4:5) at 84 K), for which the observed emission was assigned to a ligand-centered phosphorescence.[15] Although the emission manifold of ***f*-3** was considerably broad compared with the very sharp emission observed for [Ru(*i*-bqn)$_3$](PF$_6$)$_2$, the observed emissions were attributed to those from the quinoline-based $^3(\pi-\pi^*)$ emissive excited state: the ^{3}MLCT excited state of ***f*-3** is expected to be very

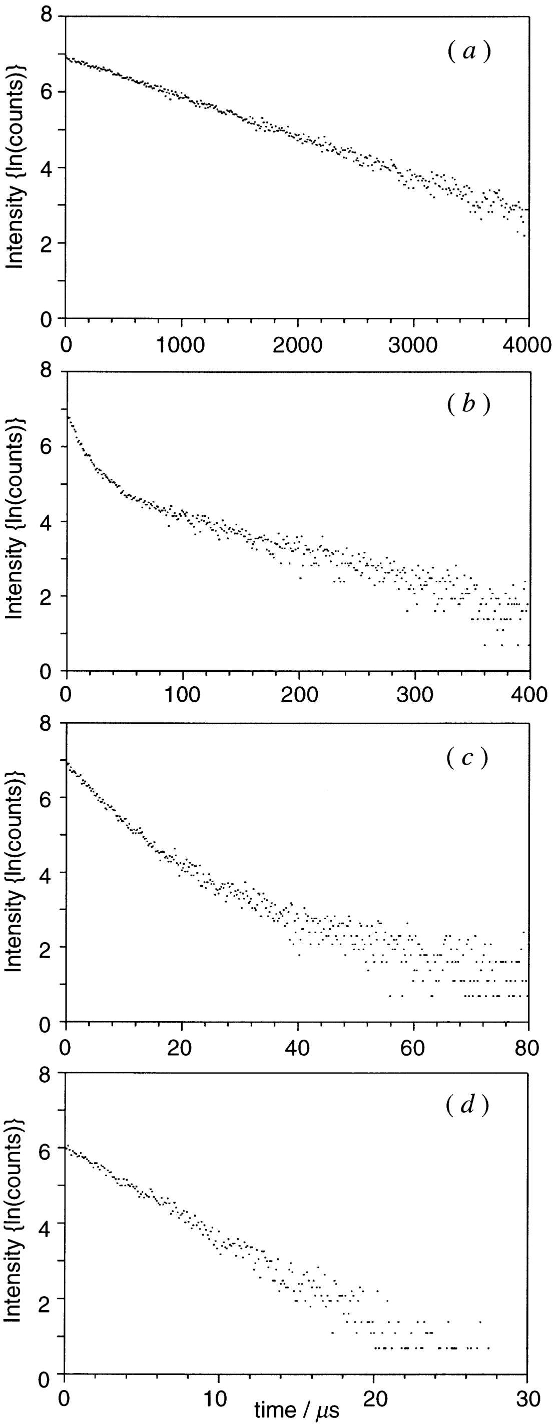

Figure 8. Emission decay of complexes (a) ***f*-3** (at 544 nm), (b) ***C*$_1$-2** (at 560 nm), (c) **1** (at 568 nm), and (d) [Ru(bpy)$_3$](PF$_6$)$_2$ (at 579 nm) in EtOH/MeOH (4:1) glass at 77 K following pulsed excitation (λ_{ex} = 337 nm). The emission decays of complexes ***C*$_1$-2** and **1** were analyzed by the following double-exponential kinetic traces: $I(t) = 713\ \exp(-t/14.6) + 141\ \exp(-t/118)$ for ***C*$_1$-2** and $I(t) = 860\ \exp(-t/6.30) + 66.2\ \exp(-t/25.3)$ for **1**.

---

(39) Kober, E. M.; Meyer, T. J. *Inorg. Chem.* **1984**, *23*, 3877−3886.

high in energy due to the strong π-acceptability of the Me_2P- donor of Me_2Pqn. The broadening of the emission manifold of ***f*-3** may be caused by the coordinated Me_2P-, although the mechanistic detail is still uncertain at this moment.

The emission spectra of the mixed-ligand complexes **1** and ***C*$_1$-2** exhibited a systematic shift of the band maximum on going from $[Ru(bpy)_3](PF_6)_2$ to ***f*-3** (Figure 7). Complex **1** exhibited an emission manifold with the highest band maximum at 566 nm and the second highest one at 600 nm (vibrational progression $\Delta\nu = 1000$ cm^{-1}) with the relative intensity of the lower energy band larger than that for $[Ru(bpy)_3](PF_6)_2$. The emisssion band maximum of ***C*$_1$-2** blue-shifted further with a broad emission envelope, which was successfully separated by the Gaussian curve-fitting analysis into two bands centered at 545 and 572 nm (the difference between these two bands was merely 870 cm^{-1}) with almost identical intensities. Similar results have already been reported for the series of mixed-ligand phosphine complexes *cis*-$[Ru(bpy)_2(P-P)]^{2+}$ ($P-P = (PMePh_2)_2$ or 1,2-bis(dimethyl- or diphenylphosphino)ethane).[22b,23] Therefore, it seems that the observed shift of the emission maximum and the change in the intensity of the low-energy band are related to the number of coordinated phosphine ligands.

The analyses of the emission lifetimes revealed that the decay follows a double-exponential function in the case of mixed-ligand complexes **1** and ***C*$_1$-2**; the emission decay of **1** at 568 nm at a temperature of 77 K exhibited a double-exponential kinetic trace that was successfully explained by lifetimes of 6.3 and 25 μs, while ***C*$_1$-2** had emission lifetimes of 15 and 120 μs (Figure 8). The analogous phen and Me_2Pqn mixed-ligand complex **1′** also exhibited a dual emission with lifetimes of 8.4 and 29 μs (the highest emission band maximum was observed at 566 nm). When such a dual emission is observed, a contribution of impurities is usually a prime suspect. However, the purity of the samples as well as the solvent is guaranteed to be very high; the solid samples were pure enough to give satisfactory results of elemental analyses, and the NMR spectra of these sample solutions indicate the absence of significant contamination. Moreover, it has been reported that the analogous Ph_2Pqn complex $[Ru(bpy)_2(Ph_2Pqn)](PF_6)_2$ also exhibited a dual emission with $\tau = 12$ and 60 μs.[36] Therefore, we believe that the observed dual emission is genuine and safely conclude that the dual emission is inherent in the Ru^{II} complexes containing 8-quinolylphosphines. By considering the extremely different emission lifetimes of $[Ru(bpy)_3](PF_6)_2$ and ***f*-3**, the longer lived component seems to originate from the quinoline-based $^3(\pi-\pi^*)$. The shorter lived emission may be assigned to the emission from the bpy-based ^{3}MLCT excited state.

The dual-emission phenomenon has rarely been observed for ruthenium(II) polypyridine complexes in solution and even in a rigid glass. In addition to the pioneering observation of a dual emission from $[Ru(bpy\ or\ phen)(Hdpa)_2]^{2+}$ (Hdpa = 2,2′-dipyridylamine) by Blakley and DeArmond,[17a] two examples have been reported; one is for the bis(bpy) complex containing 3-(pyrazin-2-yl)-1,2,4-triazolate (pztr), $[Ru(bpy)_2(pztr)]^+$,[18] and the other is for the $[Ru(bpy\ or\ phen)_3]^{2+}$-type complexes with a pendant arene (pyrene) group attached to the coordinated bpy or phen ligand.[19] For the dual emission of $[Ru(bpy\ or\ phen)(Hdpa)_2]^{2+}$, Blakley and DeArmond postulated that an interligand charger-transfer process ($n_{Hdpa}-\pi_{bpy}$* or $n_{Hdpa}-\pi_{phen}$*) is the origin of the second emission, in addition to the first emission from the ^{3}MLCT excited state.[17a] Vos et al. explained that the dual emission of $[Ru(bpy)_2(pztr)]^+$ is due to the presence of the bpy-based ^{3}MLCT and the pyrazine-based ^{3}MLCT emitting states, both of which weakly couple to each other.[18] In the complexes with an attached pendant arene group, the dual emission was attributed to the energy transfer from the bpy-based ^{3}MLCT to the arene-based $^3(\pi-\pi^*)$ excited states.[19] The dual-emission phenomena observed for the Me_2Pqn complexes are, therefore, different from those reported previously; the quinoline-based $^3(\pi-\pi^*)$ state of 8-quinolylphosphines is the origin of the relatively long lived emission.

Conclusion

A series of mixed-ligand Ru^{II} complexes with Me_2Pqn, $[Ru(bpy)_{3-n}(Me_2Pqn)_n]^{2+}$ ($n = 1$, 2, or 3), were successfully synthesized and structurally and spectrophotometrically characterized. It was elucidated that the strong *trans* influence of the Me_2P- donor in Me_2Pqn elongates the *trans*-positioned Ru^{II}−ligator bond, even the mutually *trans* Ru−P bonds. We also found that the *trans(P)*- and *mer*-isomers with mutually *trans* P−Ru−P bonds undergo photochemical conversion to produce *C*$_1$- and *fac*-isomers, respectively.

It is suggested by comparison of the electrochemical and spectroscopic properties between ***C*$_1$-2** and **4** that the electronic differentiation of Me_2Pqn does not affect the ground-state properties of the mixed-ligand Ru^{II}(bpy)-type complexes (Tables 3 and 4). However, in contrast to the emission of complex **4** that obeys a single-exponential kinetics with $\tau = 21$ μs (emission band maximum at 572 nm), complex ***C*$_1$-2** exhibited a novel dual emission with $\tau = 15$ and 120 μs. The shorter lived emission of ***C*$_1$-2** and the single emission of complex **4** were attributed to the relaxation from the bpy-based ^{3}MLCT excited state.[10,23,39] The longer lived emission of complex ***C*$_1$-2** probably originates from the quinoline-based $^3(\pi-\pi^*)$ emissive excited state, since ***f*-3** exhibited an intense emission in the same energy region as that of ***C*$_1$-2** with an extremely long lifetime ($\tau = 920$ μs). We also observed dual emission even in the cases of the mono(Me_2Pqn) complexes **1** and **1′**, as well as $[Ru(bpy)_2(Ph_2Pqn)](PF_6)_2$.[36] In contrast, analogous 8-quinolate (quo) complex $[Ru(bpy\ or\ phen)_2(quo)]PF_6$ exhibited merely a single-exponential ^{3}MLCT emission with a large red shift.[20] Therefore, the characteristic dual emission of the present 8-quinolylphosphine (R_2Pqn) complexes should be related to the phosphine group attached to the quinolyl group; the strong π-acceptability of the phosphine stabilizes the Ru^{II} dπ orbitals, inducing the shift of the bpy-based ^{3}MLCT excited states to a higher energy. We suppose that this dπ interaction causes the bpy-based ^{3}MLCT level almost isoenergetic to the quinoline-based $^3(\pi-\pi^*)$ excited state in the case of mixed-ligand R_2Pqn and bpy complexes. We, therefore, concluded that not the effect of electronic differentiation of the R_2Pqn bidentate ligand but the specific donor/acceptor property of the R$_2$P− moiety controls the characteristic dual emission of Ru^{II} complexes with R$_2$Pqn.

Acknowledgment. We are grateful to Dr. Koichi Nozaki (Osaka University) for valuable discussion about the photophysics of Ru^{II} complexes.

Supporting Information Available: X-ray crystallographic files, in CIF format, for **1**, ***tP*-2**, ***m*-3**, and ***f*-3**. This material is available free of charge via the Internet at http://pubs.acs.org.

IC020344L